

## Research Article

Bagadi Ravi Kiran\*, Vatsavayi Valli Kumari, and KVSVN Raju

# Model for High Dynamic Range Imaging System Using Hybrid Feature Based Exposure Fusion

<https://doi.org/10.1515/jisys-2018-0412>

Received Oct 13, 2018; accepted Aug 14, 2019

**Abstract:** The luminous value is high for many natural scenes, which causes loss of information and occurs in dark images. The High Dynamic Range (HDR) technique captures the same objects or scene for multiple times in different exposure and produces the images with proper illumination. This technique is used in the various applications such as medical imaging and observing the skylight, etc. HDR imaging techniques usually have the issue of lower efficiency due to capturing of multiple photos. In this paper, an efficient method is proposed for HDR imaging technique to achieve better performance and lower noise. The Luminance-Chrominance-Gradient High Dynamic Range (LCGHDR) method is proposed to obtain the proper luminous value of images. The same scenario is captured at different exposure are processed by the proposed method. Based on these feature values extracted from the different images and exposure fusion technique was developed that helps for the proper imaging. This experiment was evaluated and analyzed by comparing with the other methods, which showed the efficiency of the proposed method. This method needs only 124.594 seconds for the computation, while existing method need 139.869 seconds for the same number of images.

**Keywords:** Exposure, Exposure Fusion, High Dynamic Range, Luminance-Chrominance-Gradient HDR

## 1 Introduction

The real world scene has the dynamic range of the higher orders of magnitude much larger than the conventional digital imaging system [1]. The details of the image lost due to the underexposure and overexposure. The single image does not provide the information of the objects due to some loss of data in the images [2]. The multiple image of the same scenario with the different exposure can provide the needed information about the image, because different exposure of the image gives the different data [3]. The advancement in the image acquisition technique helps to overcome the issues present in the current imaging system and capture the scene with the higher value of dynamic range in the image from the exposure between the bright and dark places [4, 5]. The photometric and colorimetric information calculated from captured images has been highly used in scientific and engineering applications like an environment evaluation, for example, Unified Glare Rating (UGR) measurement for office or road monitor, medical imaging and graphics rendering consists of image-based lighting.

Many approaches proposed to capture the image with the proper dynamic range and some methods measure luminance to capture the HDR image [6]. The basic method is to capture the image simultaneously with

\*Corresponding Author: **Bagadi Ravi Kiran:** Andhra University College of Engineering, Visakhapatnam, Andhra Pradesh, India-531162; Email: brk2007@gmail.com

**Vatsavayi Valli Kumari:** Andhra University College of Engineering, Visakhapatnam, Andhra Pradesh, India; Professor-Department of CS&SE, Andhra University college of Engineering; Email: vallikumari@gmail.com

**KVSVN Raju:** Gayatri Vidya Parishad College for Degree and PG Courses, Rushikonda, Visakhapatnam, Andhra Pradesh, India, 530 045; Email: kvsrn.raju@gvptc.edu.in

the different exposure and then irradiance spatial dimensions of the same scenario [7]. The captured images mapped to an HDR based efficient image reconstruction algorithm [8]. The exposure time of the camera depends on the lens aperture, shutter speed, and International Organization of Standardization (ISO) levels; the exposure time controls the intensity of the light incident on the image sensor [9]. The long exposure time capture the dim details, whereas the bright area details captured using the short exposure time [10]. So, this is difficult to provide the proper illumination image without noise by the previous methods in HDR imaging. In this research, a Luminance-Chrominance-Gradient High Dynamic Range (LCGHDR) used for the effective HDR imaging technique and to reduce noise in the image. This method extracts the Luminance, chrominance and gradient value from the different exposure images and it produces the image with proper exposure. The proposed HDR method compared with state-of-art methods such as BAR, AEE, false position and secant for the evaluation purpose in the manner of efficiency and Signal to Noise Ratio (SNR). The proposed method have the higher efficiency in fusing the image and provide the HDR image with high quality and low computational time. The proposed method showed higher performance compared to the other method.

## 2 Literature review

Current research technologies in the HDR imaging were reviewed in this section. This gives the current techniques in the HDR imaging and also their advantages and limitations for the respective research.

Xiaomin Wu, *et al.* [11] created a colorimetric method for the reconstruction in CIEXYZ with the camera device implementation to attain the accurate colorimetric and luminance information of the HDR scene. The colorimetric characterization transformed the individual RGB values of the picture into the related to CIEXYZ values with unlimited capture. The weighing function calculated according to the value of characterization accuracy fused with XYZ values. The performance was verified by the two phases of experiments and under the constant relative Spectral Power Distribution (SPD) of lighting it outperformed the traditional ones, it has 2 CIELAB units less than the traditional one and in the illuminations of different Correlated Color Temperatures (CCTs) is 3.5 CIELAB. The HDR reconstruction under mixed lighting conditions uses a standard color checker.

Qingsen Yan, *et al.* [12] utilized the sparse representation framework to remove ghost from the HDR image using the synthesis algorithm. The ghost artifacts created due to the adjacent Low Dynamic range (LDR) image and the moving object sparsity. The problem formulated into the two processes, those are, detection of moving object and ghost free HDR generation. The proposed method has the higher performance than the existing methods based on the textures and colors. The overall performance of this technique was better and in the few databases, the value of the Peak Signal to Noise Ratio (PSNR) was less than those other methods.

Yuije Wu, *et al.* [13] established the calibrated embedded system for quasi real-time lighting for HDR sky monitoring. The direction of the device was set in direct of a test module with unilateral-facades to calculate the distribution of the luminance in sky and the ground dome. The measurement of the luminance distribution made for the sun, landscape and ground dome, and on-board luminance processed on the device. This proposed method and the Perez all-weather sky model was compared and this method attained the more reliable, which had the 10%-25% more accuracy due to HDR imaging and luminance mapping in transient lighting computation of horizontal luminance. This can possibly help to improve the system that rejects the sun's component in the luminance map.

Yang Song, *et al.* [14] proposed exposure condition analysis method depends on the quality evaluation method for the tone-mapped HDR images. First, local exposure property is analyzed for the segmentation of HDR exposure model that used to separate image. The two new quality features such as abnormal exposure ratio and exposure residual energy extracted. The color-based feature was also extracted from the different exposure region. The quality evaluation model implemented by regression training. The ability of the model to calculate the quality of tone-mapped HDR images showed in their experiment. The Pearson linear correlation coefficients are higher than 0.88; this technique has the high consistent with human visual perception.

Hyuk-Ju Kwon, *et al.* [15] proposed the new method in the HDR blending algorithm, which used only the dual-exposure image. The least squares method used in the proposed algorithm and it also included the

spatial and intensity weighting functions. The error point was reduced and improved the function of camera response using the weighting function. In addition, a constraint was added to correct the white balance in the brightness level. The result showed that the proposed technique outperformed the existing methods. This method was not evaluated in the real time function and this gives the efficiency of the system.

The importance of the luminance property of HDR method is shown in the research [11] and [13]. The sparse value of the image is very useful in HDR imaging and for ghost elimination in HDR [12], which may contain some noise. The quality measure based on texture and color was proposed in [14], and this method limited to preserving the image. The luminance property alone cannot provide higher efficiency and other feature are need to be extracted. However, the quality of the images produced by the existing method is not efficient for practical use and loss in the images are high. The existing method features is not involves in preserving the image quality. The existing method doesn't use the combination of the luminous, chrominance and gradient features. The proposed method differ from the existing method in the form of three features extraction such as Luminous, Chrominance and Gradient. These features are fused to provide the proper luminous in HDR image. These limitations in HDR imaging method are overcome by proposing LCGHDR method and increase the efficiency of HDR.

## 2.1 Limitations of Previous studies

The sparse representation framework [12] has better performance in HDR imaging. However, this does not provide the HDR with high quality. This tends to loss in the details of the image. The existing method still lacks in the provide the output images with less noise. The computation time is another factor is need to be considered. The studies in the survey [11–15] doesn't show much efficiency in the quality of the image. The new technique is required to effectively perform the HDR function without affecting the image quality. The comparison of the HDR imaging methods is shown in Table 1.

**Table 1:** Comparisons of previous studies

Author(s)	Methods	Datasets	Advantages	Limitations	Performance evaluation
Xiaomin Wu, <i>et al.</i> [11]	colorimetric characterization	Simulated data	The color is reconstructed effectively.	Need to develop the method for mixed lightning condition.	Average luminous value = 1.33.
Qingsen Yan, <i>et al.</i> [12]	Sparse Representation	Door, arch and sculpture garden dataset.	Fusion is performed without artifacts.	The quality of the output image is not high.	PSNR = 16.12.
Yujie Wu, <i>et al.</i> [13]	Calibrated Embedded System	Simulated data	Accuracy is high in this method.	The output image are having high luminous value and affects the details of images.	Relative error = 11%.
Yang Song, <i>et al.</i> [14]	Tone mapping based on exposure	Tone-mapped Image Database (TMID)	Error value is low in this method.	The accuracy of the method is need to be increased.	RMSE = 0.8342.
Hyuk-Ju Kwon, <i>et al.</i> [15]	Spatial and intensity correlation	Simulated dataset	The color distortions is reduced.	The higher exposure image is need to be considered.	-

### 3 Proposed method

The images from the database used as an input and the features such as luminance, chrominance and gradient were extracted from those images. An exposure fusion technique was developed based on the features and provide the image with the proper luminance. The higher luminance image and lower luminance images used as input. The experimental result compared with other existing method in the HDR imaging. The flow chart of the LCGHDR method is shown in the Figure 1. The illustration of the dataset and algorithm of this method is given below.

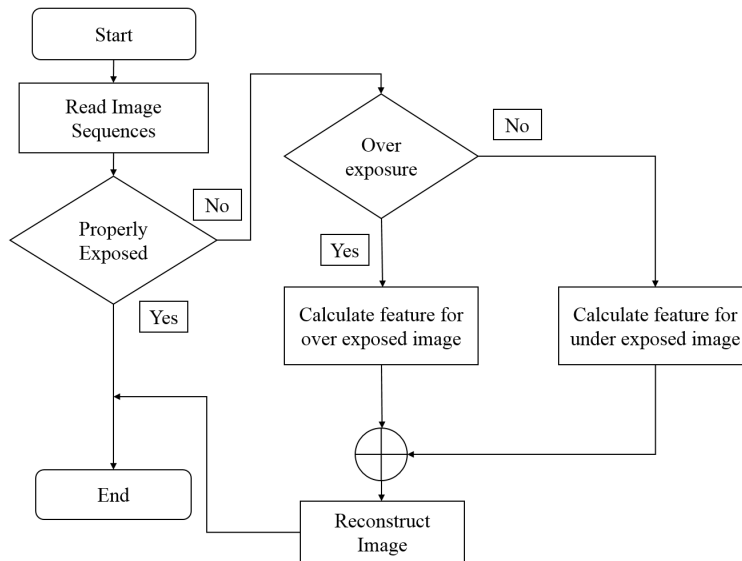


Figure 1: The flow chart of LCGHDR method

#### Pseudo code

1. Begin
2. Read image \\the input images with high exposure  $I_H$ .
3. Check whether the scenario is under exposure, over exposure or proper exposure using the mean luminance value of the image. The mean luminance value of the image is 0 to 100 is under exposed, 100 to 150 is properly exposed and 150 above is over exposed.
4. If over exposed
  - a.  $L_H = L$
  - b. Measure  $L$ ,  $C$  and  $G$ . \\Measure the mean value of high exposure image  $L_H$ .
  - c. Fuse  $L$ ,  $C$  and  $G$ .
5. If Else Lower exposed
  - a.  $L_L = L$
  - b. Measure  $L$ ,  $C$  and  $G$ ;
  - c. Fuse  $L$ ,  $C$  and  $G$ ;
6. Else
  - a.  $L = L$ ;
7. End
8. End

The input images is measured in terms of exposure value. If the input images is under expose and lower exposure, then measure the luminous, chrominance and gradient value. Fuse the value to provide the proper exposure image with other exposure image.

### A. Database collection

The HDR Photographic Survey is the exclusive HDR database and consists of detailed colorimetric/luminance measurements [16]. The images have the contents and challenges with the data for the HDR algorithm. This is a publicly available database and this can be followed for the non-commercial research purpose. The attempt was made to collect the datasets up to 40 images and having 106 images in total by now. Twenty-eight images in the database have been accompanying colorimetric, appearance data and the several data associated with the remaining data in the images. The thumbnail is available in the database to view the image and the images can be downloaded in the OpenEXR file. The database size is more than 13GB and this database inspired from the nineteenth century photographic survey of the American west. This database and stimulated database used to understand the performance of this method. Figure 1 shows the sample images from the database. Apart from this, simulated dataset are used. The ten scenes were captured with different exposure for each scene.

### B. Exposure Fusion

The luminance, the two chrominance and gradient components are denoted as  $Y$ ,  $U$ ,  $V$ , respectively. Let  $z = [z_R, Z_G, Z_B]$  be an image in the RGB space and  $\zeta = [\zeta_Y, \zeta_U, \zeta_V, \zeta_G]$  is the same images in the luminance, chrominance and gradient space. The RGB value of the image are denoted in Roman letters and gradient values are denoted in Greek letters. The transformation of the image from the RGB to the manner of luminance, chrominance and gradient is defined in the matrix form as  $\zeta = zA$ , where  $A$  is the matrix normalized in such a way that if  $z(-) \in [0, 1]^3$ , then  $\zeta(-) \in [0, 1] \times [-0.5, 0.5]^2$ . The hue and saturation can be defined as  $H = \arctan \frac{\zeta^U}{\zeta^V}$  and  $S = \sqrt{(\zeta^U)^2 + (\zeta^V)^2}$ , respectively.

Consider a set of images  $\zeta_i = [\zeta_i^Y, \zeta_i^U, \zeta_i^V, \zeta_i^G, i = 1, \dots, N]$  in the luminance-chrominance-gradient space, captured with different exposure time  $\Delta t_i$  and with LDR, assuming  $\zeta(x) \in [0, 1] \times [-0.5, 0.5]^2$ , where  $X = [x_1, x_2]$  is a pixel representation. The objective is to obtain the single HDR image  $\tilde{\zeta} = [\tilde{\zeta}^Y, \tilde{\zeta}^U, \tilde{\zeta}^V, \tilde{\zeta}^G]$  in the same color space. In this method, the luminance, chrominance and gradient values are processed separately.

#### 1. Luminance component composition

The multiple images captured from the same scenario with the different exposure times used to calculate the luminance channel. The sufficient amount of pixels is taken with increasing monotonical values between under and over-exposure images. Using these pixels, the camera response function is fitted and applied an Singular Value Decomposition (SVD) solver. In this research, 100 pixels are considered as sufficient in most cases. The camera response measured only once and used for the input values as linearization in all HDR compositions of the same device.

The HDR luminance component calculated by a pixel wise weighted average of input luminance and as a weighting function, Gaussian function with a mean of 0.5 and a standard deviation of 0.2 thus ensuring a smaller impact of the under or over-exposed pixels. The calculation of the logarithmic HDR luminance obtained as Eq. (1).

$$\ln \tilde{\zeta}^Y(x) = \frac{\sum_{i=1}^N \omega^Y(\zeta_i^Y(x))(g(\zeta_i^Y(x)) - \ln \Delta t_i)}{\sum_{i=1}^N \omega^Y(\zeta_i^Y(x))} \quad (1)$$

From the Eq. (1), is the camera response function and the value of the HDR luminance is measured in the logarithmic scale. After applying the natural exponential, the resulting values are positive, normally spanning  $[10^{-4} 10^4]$  thus being truly HDR.

## 2. Chrominance component composition

There is no camera response required for the chrominance components and the color saturation is taken for the weight the chrominance. If the value of the color saturation is high in the image, that means the valuable chromatic information is present in more pixel and the weight is higher. More specifically,  $\omega^{UV}(S) = S^\alpha$ , where  $1 > \alpha < 2$ . In this method, we found that  $\alpha = 1.5$  is a good choice. The mean value is set when the pixel is over and under exposed, it will less saturated than the correct exposure. The mean value is less than one is under exposed and more than two involves in over-exposed. In order to preservation of color in the image, the same weight is used for the both chromatic components and compose any chromatic component  $C \in \{U, V\}$  as Eq. (2).

$$\tilde{\zeta}^C(x) = \frac{\sum_{i=1}^N \omega^{UV}(S_i(x)) \zeta_i^C(x)}{\sum_{i=1}^N \omega^{UV}(S_i(x))} \quad (2)$$

Where  $S_i$  denotes the saturation of  $\zeta_i$ . Bearing a convex combination of the input chrominances, the range of  $\tilde{\zeta}^C(x)$  is again in  $[-0.5, 0.5]$ . The distinct pixel value possible number is greater than in the original source sequence.

## 3. Gradient value of the image

The weighted map of the gradient information is generated for static and dynamic scenario and similarly to Canny detection, the first derivatives of 2-D Gaussian filter  $g(x, y; \sigma_d)$  in the x- and y- directions to extract the gradient information is given in the Eq. (3) & (4).

$$I_x^i(x, y) = I^i(x, y) \otimes \frac{\partial}{\partial_x} g(x, y; \sigma_d) \quad (3)$$

$$I_y^i(x, y) = I^i(x, y) \otimes \frac{\partial}{\partial_y} g(x, y; \sigma_d) \quad (4)$$

Where  $I_x^i(x, y)$  and  $I_y^i(x, y)$  are the partial derivatives of image  $I^i(x, y)$  along the x- and y- directions, respectively. Standard deviation  $\sigma_d$  is set to two pixels in the experiments and the gradient magnitude reflects the maximum change in pixel values, whereas the angle points out the direction related to the maximum change. These two components calculated in the following Eq. (5).

$$\tilde{\zeta}^G(x, y) = \sqrt{|I_y^i(x, y)|^2 + |I_x^i(x, y)|^2} \quad (5)$$

The luminance, chrominance and the gradient values used to develop for exposure fusion and this provide the image with proper illumination. The brief description of the fusion method using the feature values is given below.

## C. Fusion Method

A luminance range reduction operator is  $T$  and define its output, the reduced-range luminance image, as  $\zeta(x) \in [0, 1]$ . This is the most effective approach in term of the chromatic channels. The sRGB gamut does not allow the rendering of the very dark or very bright and saturated colors, which is present in the real scenes and captured in the HDR images. Therefore, there is a need for a chromatic feature and hue intact while sacrificing saturation in order to fit into the sRGB gamut. Introducing a scaling factor  $\delta$  for the two chrominance will scale

down the saturation and not change the hue. The scheme is used to guarantee sRGB values present in color space transformation itself, which is described as follows.

Let  $B = A^{-1}$  be the luminance, chrominance and gradient to RGB transformation matrix and define the gray (achromatic) image and its chromatic complement image in RGB space by

$$z_{gray}(x) = [z_{gray}^R(x) z_{gray}^B(x)] = \begin{bmatrix} T(\tilde{\zeta}^Y(x)) \\ 0 \\ 0 \end{bmatrix}^T B.$$

$$z_{chrom}(x) = [z_{chrom}^R(x) z_{chrom}^G(x) z_{chrom}^B(x)] = \begin{bmatrix} 0 \\ \tilde{\zeta}^U(x) \\ \tilde{\zeta}^V(x) \end{bmatrix}^T B.$$

$$\dot{z}_{grad}(x) = [\dot{z}_{grad}^R(x) \dot{z}_{grad}^G(x) \dot{z}_{grad}^B(x)] = \begin{bmatrix} T(\tilde{\zeta}^G(x)) \\ 0 \\ 0 \end{bmatrix}^T B.$$

Remark that  $z_{gray}(x)$  is truly a gray image because in RGB to luminance, chrominance and gradient transforms  $b_{1,1} = b_{1,2} = b_{1,3}$ . Look for a map  $\delta \geq 0$ , calculated in the Eq. (6) and (7).

$$\dot{z}(x) = \dot{z}_{gray}(x) + \delta(x) z_{chrom}(x) \in [0, 1]^3 + \dot{z}_{grad}(x) \quad (6)$$

This can be define by  $\delta(x) = \min\{1, \delta_R(x), \delta_g(x), \delta_B(x)\}$

$$\delta_R(x) = \begin{cases} \frac{z_{gray}^R(x)}{-z_{chrom}^R(x)} & \text{if } z_{chrom}^R(x) < 0 \\ \frac{1-z_{gray}^R(x)}{z_{chrom}^R(x)} & \text{if } z_{chrom}^R(x) > 0 \\ 1 & \text{if } z_{chrom}^R(x) = 0 \end{cases} \quad (7)$$

Where  $\delta_g$  and  $\delta_B$  are defined analogously. Thus,  $\delta$  is the largest one, which allows the condition (1) to hold. It is easy to realize that the hue of  $z(x)$  is not influenced by  $\delta$ , whereas the saturation is measured proportionally to it. The low dynamic range image  $z(x)$  has colors which consists of the same hue as those in the HDR image  $\tilde{\zeta}$  and which are desaturated a little, as it needed to fit within the sRGB gamut.

The fused image can be defined in the Eq. (8) with luminance, chrominance, and gradient space as

$$\dot{\zeta}(x) = [T(\tilde{\zeta}^Y(x)) \delta(x) \tilde{\zeta}^U(x) \delta(x) \tilde{\zeta}^V(x) T(\tilde{\zeta}^G(x))] \quad (8)$$

The luminance, chrominance and gradient image  $\zeta$  can be compressed and stored directly with an arbitrary method and for display transformed into RGB using the matrix B. This method evaluated and its performance presented in the experimental result section.

## 4 Experimental Result

The experiment conducted in the software of MATLAB (R2017b) with the system specification of 4GB of RAM and 3.0 GHz processor. The value of iteration was set at 50 and the various images with different exposure considered as input and process the image. The iteration value above 50 is static for almost every image in the dataset. Hence, the iteration value is set as 50. The output obtained as a properly illuminated image and that image took for the evaluation. This method was evaluated in terms of efficiency and Signal to Noise ratio (SNR). The other existing methods were also processed in the same dataset and compared it with the proposed method. The database has the same images with different illumination and it consists of the few sets of images. The proposed method is evaluated with the existing method in the same hardware resources with same images. Each set of images have the fifteen similar image capture in the different exposure. The HDR techniques used for the 10 set of images and obtain the image with proper illumination.

The input images obtained from the HDR Photographic Survey dataset and 106 images are used as an input image for evaluation. The feature values such as luminance, chrominance and gradient values extracted from the images. The fusion technique was developed based on the feature value and it provided the proper illumination measure. The two input images of the HDR Photographic Survey database are shown in the Figure 3 (a) & (b) with the high illumination in 3 (a) and low illumination in 3 (b) for three images like living room, lawn, and forest respectively. The output image with the proper illumination is given in the Figure 3 (c). The two input images of stimulated dataset are shown in the Figure 4 (a) & (b) for three images such as building 1, building 2 and park, the output of respective image is shown in the Figure 4 (c).



(a)



(b)

**Figure 2:** HDR Photographic Survey (a) Ahwahnee Great Lounge image with low luminance (b) Zentrum image with low luminance



**Figure 3:** Sample image of building from Stimulated database

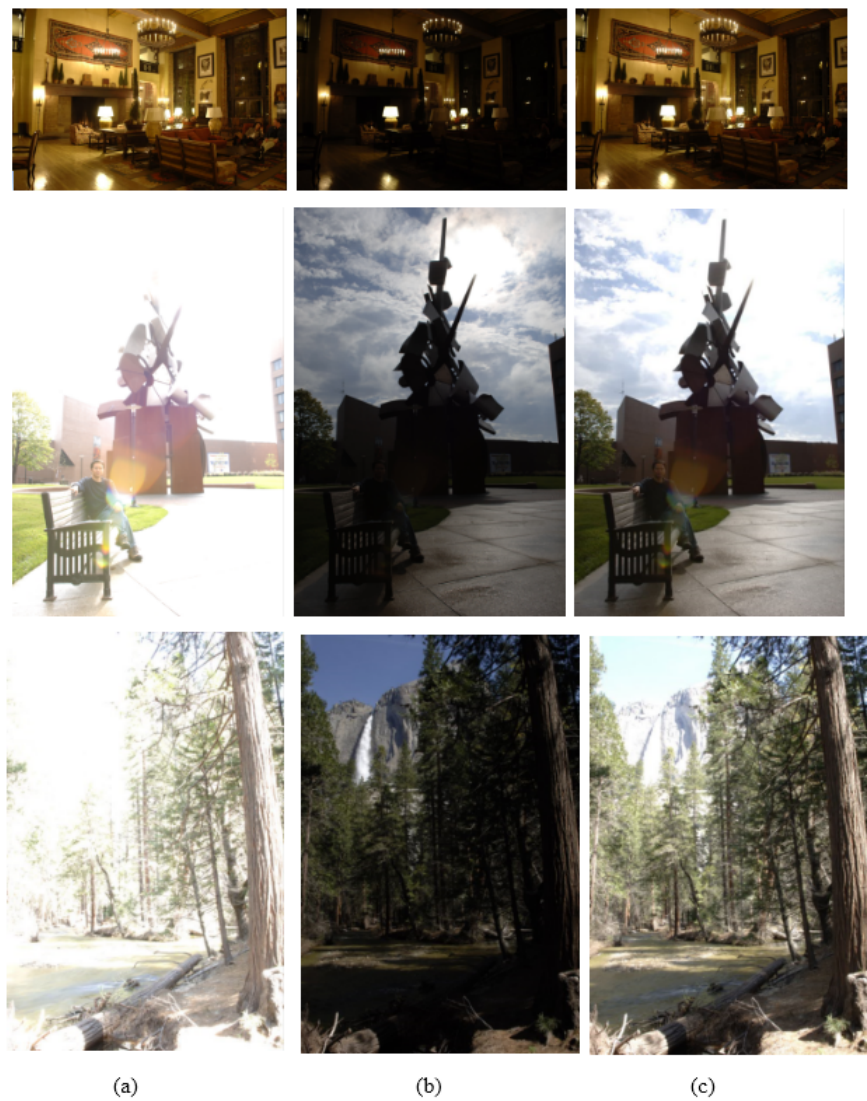


**Figure 4:** (a) Input image with high luminance (b) Input image with low luminance (c) output image

#### A. Performance evaluation in HDR Photographic Survey database and Simulated database

The BAR and Adaptive Exposure Estimation (AEE) [17] were compared with the LCGHDR to analyze its function in the manner of percentage of lost, shots, and Time efficiency (Table 1). The proposed method showed higher performance in terms of the time compared to the other two methods (BAR and AEE). The BAR method uses the three shots of the picture for HDR, and LCGHDR, AEE uses two shots. The pixel lost value denoted as a percentage of the pixel lost in fusion technique, which measured from the comparison of input and output image. Some captured images of lost value are equal to zero, which shows no loss in the fusion technique. The time efficiency  $\sum_{i=1}^N T_i(s)$  is the total time computation for the exposure fusion with total number of caption. The LCGHDR method requires only two captured images and less time for the HDR imaging. In Simulated database, the ten scenes were captured in total and there are 15 images with different illumination is captured for each scene and used for HDR imaging. In HDR photographic survey database, the BAR method need 218.734 seconds for the 96 images and AEE method took total 81 images in 139.869 seconds. The proposed method requires 124.594 seconds for the 81 images.

The mean luminous value for the five images from the simulated dataset are shown in the Table 2. The Mean luminous value of the two inputs and one-output images for the five images presented in the Table 2. The mean value of the highly exposed input images having the higher luminance value and for the low exposed image has the low luminance value. These images used to measure the feature values and exposure fusion helps to produce the image with a proper illuminant value.

**Table 2:** Comparison of BAR, AEE and LCGHDR

Number of scene	Methods	Number of shots	% Lost	$\sum_{i=1}^N T_i(s)$
1	BAR	3	1.61	0.301
	AEE	2	1.61	0.025
	LCGHDR	2	1.61	0.014
2	BAR	3	0	0.301
	AEE	2	0	0.101
	LCGHDR	2	0	0.85
3	BAR	3	0	0.301
	AEE	2	0	0.04
	LCGHDR	2	0	0.021
4	BAR	3	0	0.301
	AEE	2	0	0.05
	LCGHDR	2	0	0.032
5	BAR	3	0	0.301
	AEE	2	0	0.034
	LCGHDR	2	0	0.015
6	BAR	3	0	0.301
	AEE	2	0	0.025
	LCGHDR	2	0	0.012
7	BAR	3	0	30.282
	AEE	2	0	13.067
	Proposed LCGHDR	2	0	11.042

Table 3 gives the PSNR value for the input images and output images. The input images are Low Dynamic Range (LDR) images and output images are fused images. The four Scenes of images used to measure the PSNR value. The two input images used for each case and average PSNR measure compared with the output images. This shows that the PSNR value for the output image is higher than the input images.

**Table 3:** Mean value for the input and output images

Scenes	Images	Mean luminous value		
		High exposed input image	Low exposed input image	Output image
Scene 1	Living room	162	95	124
Scene 2	Forest	168	92	112
Scene 3	Building 1	184	72	134
Scene 4	Building 2	173	93	132
Scene 5	Park	167	82	121

### B. Signal to Noise Ratio

The SNR is measured for this method and compared it with other methods. In the AEE method, the four different conditions made for comparative purpose namely A (LO = 3 and HI = 253), B (LO = 16 and HI = 240), C (LO = 56 and HI = 200), and D (LO = 106 and HI = 150). The proposed LCGHDR has been compared with the AEE method with four different conditions, BAR method and Ground Truth (GT) images. The SNR value is measured by ratio of HDR value () over the standard deviations (). The SNR values measured using the Eq. (9) and shown in the Table 4.

$$SNR_{xy} = 20 \times \log_{10} \left( \frac{\bar{E}_{xy}}{\sigma_{xy}} \right) \quad (9)$$

**Table 4:** PSNR value for the images

Images	Average PSNR value of input image	Output image PSNR value
Scene 1	24.24	28.51
Scene 2	25.74	30.54
Scene 3	22.15	27.94
Scene 4	24.78	28.78

The proposed LCGHDR method has been compared with the other methods and AEE method with four different conditions, shown in Table 4. The number of shots is given in the table with the total computation time. The proposed method has the better SNR performance compared to the other method. The number of shots of the proposed method is four and compared it with other methods. This provides high performance compared to the other methods.

The graphical representation of the SNR values for the different method presented in the Figure 5. The AEE method evaluated in the four different conditions and compared it with the proposed system. The proposed system utilizes the four shots for its function and has higher SNR value compared to the other methods.

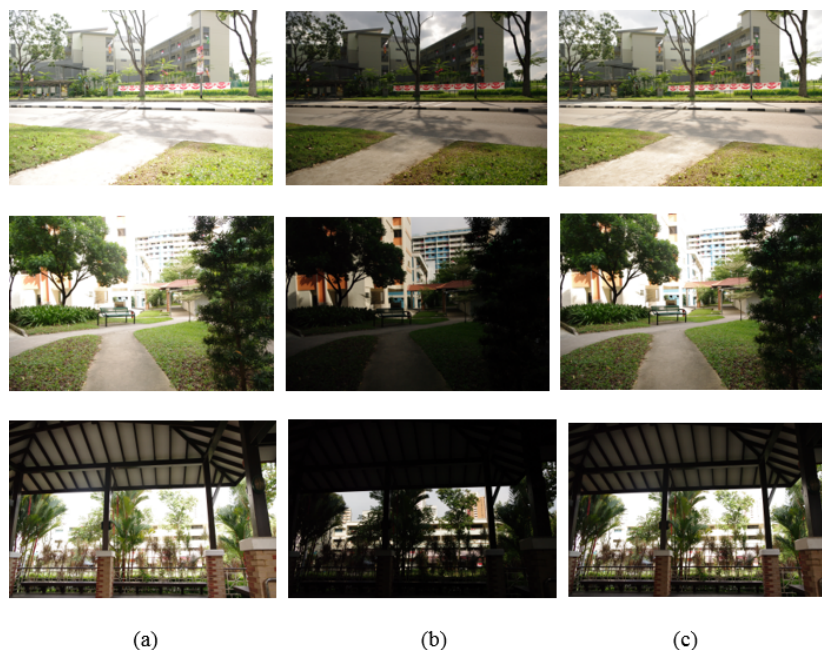


**Figure 5:** Stimulated dataset (a) High exposure Input image (b) Low exposure Input image (c) Output image with proper exposure

### C. Evaluation in Stimulated dataset

LCGHDR has been compared with six methods in terms of control time in HDR imaging with seconds is shown in Table 5. The four cases evaluated for the processing these six existing methods and the mean value is calculated. The control time stopped if the process takes more than 20 seconds for the processing. The HDR image is need to be processed in less time and techniques required more than 20 second to process HDR is not applicable for the practical purposes [19]. The false prediction method requires more time for processing the four cases as well as the Secant, Bisection and Kuno. The false prediction having the large time for the HDR imaging of exceeding 20 seconds, Kuno has lower time of 0.08 seconds. The secant also has the exceeding 20 seconds and Bisection requires 0.48 seconds. The proposed method needs only less time for the computation except Kuno. But Kuno and Liang method often fails in processing the images. The Kuno method is not iteration method, so convergences techniques is not applied that tends to create exposure error in the image. The Liang method on the other hand doesn't considered the underexposed part. As the results, this will create tumbling effort in the most of the image. The Liang method has higher efficiency in time compared to all other method and it causes a tumbling effect in its functions.

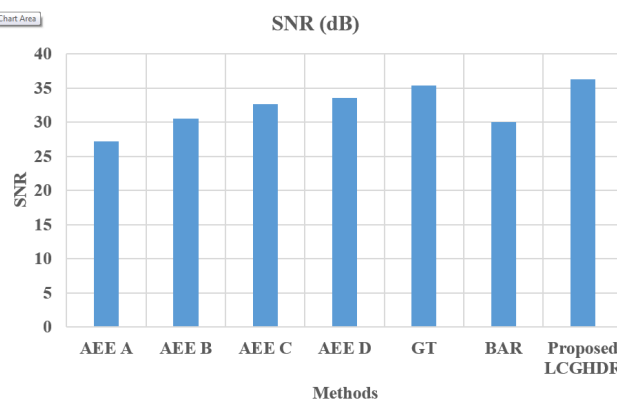
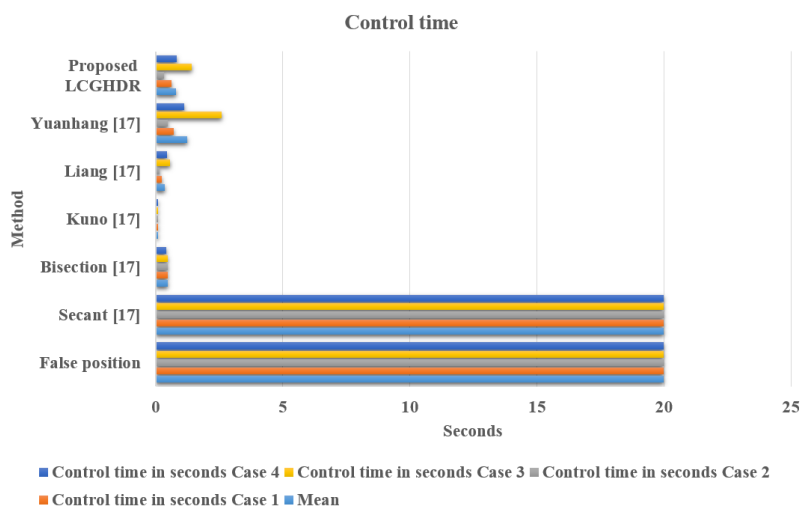
**Table 5:** SNR value for the different method

Methods	Number of shots	$\Delta t(s)$	SNR (dB)
AEE A [17]	3	14.79	27.19
AEE B [17]	4	15.02	30.47
AEE C [17]	5	31.32	32.58
AEE D [17]	16	61.22	33.57
GT [17]	55	151.43	35.32
BAR [18]	4	30.3	29.97
Proposed LCGHDR	4	12.58	36.27

**Table 6:** Control time in seconds for several methods

	Control time in seconds				
	Mean	Case 1	Case 2	Case 3	Case 4
False position [19]	20	20	20	20	20
Secant [19]	20	20	20	20	20
Bisection [19]	0.48	0.48	0.48	0.48	0.4
Kuno [20]	0.08	0.08	0.08	0.08	0.08
Liang [21]	0.35	0.24	0.16	0.56	0.44
Yuanhang [19]	1.23	0.72	0.48	2.6	1.12
Proposed LCGHDR	0.795	0.63	0.32	1.4	0.83

The graphical representation of the control time of the six methods showed in the Figure 6. The false prediction method and Secant method require more than 20 seconds for image fusing. If any method performs more than 20 seconds, then it stops immediately. The remaining method has the least time for the HDR imaging and Kuno have the very less time for its function. There are four cases used to evaluate the performance of the methods in the manner of the time (seconds). The proposed system showed the efficient time for the processing of HDR imaging except Kuno and Liang. But, Kuno often fails in the processing and Liang has the higher tumbling effects in their process.

**Figure 6:** SNR comparison**Figure 7:** Control time

#### D. Comparison Analysis

The comparison has been done between the proposed LCGHDR method and existing method in terms of control time. The LCGHDR method and existing methods are processed in the same hardware resources and the parameter is measured. The total computation time is measured for both existing and LCGHDR methods, which is shown in Table 6. The proposed LCGHDR achieved the notable result in the HDR technique compared to other methods. The area-based method was followed in the research [22] and high probability error occurred in this method due to poor specular detection. The study [23] used sigmoid-based mapping curve method and gamma expansion method was evaluated in the research [24]. Gwon Hwan An, *et al.* [25] proposed a method based on the tone mapping, which uses the adaptive specular region to identify the bright and dark region. This technique achieved high quality image using final mapping decision method with low execution time. The discrete cosine transform technique was used to generate the residual data and created the backward compatible image coding method for HDR [26]. In Table 6 the LCGHDR method is compared with other methods and shows that this technique is process with low computational time.

**Table 7:** Computational time analysis of various HDR method

Different techniques	Computational time
Meylan <i>et al.</i> [22]	1.2153
Huo <i>et al.</i> [23]	1.4100
Masia <i>et al.</i> [24]	0.9955
Gwon Hwan An, <i>et al.</i> [25]	0.6599
Seungcheol Choi, <i>et al.</i> [26]	1.3505
HDRCloudSeg [27]	0.6241
LCGHDR	0.5826

**Table 8:** Computation complexity of different methods

Method	Computation Complexity
False position	$O(n \log n)$
Secant	$O(n^3)$
Bisection	$O(n \log n)$
Kuno	$O(n^2)$
LCGHDR	$O(\log n)$

### E. Computation Complexity

The computation complexity of the LCGHDR method is measured as  $O(\log n)$ . The computation time increases as the size of input increases. The proposed method is highly based on the pixel value of the image. Hence, the computational complexity is derived as  $O(\log n)$ .

This experimental result clearly showed that the proposed LCGHDR method has higher efficiency and higher SNR values. From the analysis, it is clear that LCGHDR technique performed using less number of captures and produced a high detailed image.

## 5 Conclusion

The HDR imaging captures multiple images and give the proper illumination of the image for better understanding of information. The loss of information may occur in the high and low exposure; this makes the HDR imaging as a more important method. The same images with different exposure are captured and analyzed for the proper illumination. Now a days HDR techniques are highly used and in the smartphone camera. The HDR imaging generally has the problem of low efficiency due to the process of capturing multiple images and analyze for better illumination. LCGHDR method requires less captures for the function of HDR, which helps in reduction of the performance time. The proposed method is evaluated on both benchmark dataset and simulated dataset. The proposed method outperformed the existing methods in the terms of efficiency and SNR. The PSNR values attained higher than the input images and this method executed in 124.594 seconds while existing method has required 139.869 seconds for execution. The future work will be removing the ghost artifacts in the HDR imaging without affecting the quality of the image.

## References

[1] S. Schulz, M. Grimm, and R.R. Grigat, “Using brightness histogram to perform optimum auto exposure,” *WSEAS Transactions on Systems and Control*, vol. 2, no. 2, p.93, 2007.

- [2] T. Grosch, "Fast and robust high dynamic range image generation with camera and object movement. Vision, Modeling and Visualization," *RWTH Aachen*, pp. 277-284, 2006.
- [3] S.C. Hsia, and T.T. Kuo, "High-performance high dynamic range image generation by inverted local patterns," *IET Image Processing*, vol. 9, no. 12, pp. 1083-1091, 2015.
- [4] S. Uda, F. Sakae, and J. Sato, "Variable exposure time imaging for obtaining unblurred HDR images," *IPSJ Transactions on Computer Vision and Applications*, vol. 8, no. 1, pp. 3, 2016.
- [5] P.J. Lapray, B. Heyrman, and D. Ginhac, "HDR-ARTiSt: an adaptive real-time smart camera for high dynamic range imaging," *Journal of Real-Time Image Processing*, vol. 12, no. 4, pp. 747-762, 2016.
- [6] I. Popadić, B.M. Todorović, and I. Reljin, "Method for HDR-like imaging using industrial digital cameras," *Multimedia Tools and Applications*, vol. 76, no. 10, pp. 12801-12817, 2017.
- [7] G.Y. Lee, S.H. Lee, H.J. Kwon, and K.I. Sohng, "Visual acuity-adaptive detail enhancement and shadow noise reduction for iCAM06-based HDR imaging," *Optical Review*, vol. 22, no. 2, pp. 232-245, 2015.
- [8] W. Sun, C. Han, X. Xue, H. Lv, J. Shi, C. Hu, X. Li, Y. Fu, X. Jiang, L. Huang, and H. Han, "An HDR imaging method with DTDI technology for push-broom cameras," *Photonic Sensors*, vol. 8, no. 1, pp. 34-42, 2018.
- [9] A.R. Várkonyi-Kóczy, S. Hancsicska, and J. Bukor, "Fuzzy information measure for improving HDR imaging," *In proceedings on Recent Developments and New Direction in Soft-Computing Foundations and Applications*, Springer, Cham, pp. 113-126, 2016.
- [10] A.G. Patil, and S. Raman, "Tone Mapping HDR Images Using Local Texture and Brightness Measures," *In Proceedings of International Conference on Computer Vision and Image Processing*, Singapore, pp. 443-452, 2017.
- [11] X. Wu, J. Fang, H. Xu, and Z. Wang, "High dynamic range image reconstruction in device-independent color space based on camera colorimetric characterization," *Optik-International Journal for Light and Electron Optics*, vol. 140, pp. 776-785, 2017.
- [12] Q. Yan, J. Sun, H. Li, Y. Zhu, and Y. Zhang, "High dynamic range imaging by sparse representation," *Neurocomputing*, vol. 269, pp. 160-169, 2017.
- [13] Y. Wu, J.H. Kämpf, and J.L. Scartezzini, "Characterization of a quasi-real-time lighting computing system based on HDR imaging," *Energy Procedia*, vol. 122, pp. 649-654, 2017.
- [14] Y. Song, G. Jiang, M. Yu, Z. Peng, and F. Chen, "Quality assessment method based on exposure condition analysis for tone-mapped high-dynamic-range images," *Signal Processing*, 2017.
- [15] H.J. Kwon, S.H. Lee, G.Y. Lee, and K.I. Sohng, "Radiance map construction based on spatial and intensity correlations between LE and SE images for HDR imaging," *Journal of Visual Communication and Image Representation*, vol. 38, pp. 695-703, 2016.
- [16] M.D. Fairchild, "The HDR photographic survey," *In Proceedings of the Color and Imaging Conference*, Society for Imaging Science and Technology, vol. 2007, no. 1, pp. 233-238, 2007.
- [17] M.A. Martínez, E.M. Valero, and J. Hernández-Andrés, "Adaptive exposure estimation for high dynamic range imaging applied to natural scenes and daylight skies," *Applied optics*, vol. 54, no. 4, pp. B241-B250, 2015.
- [18] Barakat, N., Hone, A.N. and Darcie, T.E., 2008. Minimal-bracketing sets for high-dynamic-range image capture. *IEEE Transactions on Image Processing*, 17(10), pp.1864-1875.
- [19] Y. Su, J.Y. Lin, and C.C.J. Kuo, "A model-based approach to camera's auto exposure control," *Journal of Visual Communication and Image Representation*, vol. 36, pp. 122-129, 2016.
- [20] Kuno, T., Sugiura, H. and Matoba, N., 1998. A new automatic exposure system for digital still cameras. *IEEE Transactions on Consumer Electronics*, 44(1), pp.192-199.
- [21] Liang, J., Qin, Y. and Hong, Z., 2007, October. An auto-exposure algorithm for detecting high contrast lighting conditions. In 2007 7th International Conference on ASIC (pp. 725-728). IEEE.
- [22] L. Meylan, S. Daly, and S. Süsstrunk, "The reproduction of specular highlights on high dynamic range displays," *In Proceedings on Color and Imaging Conference*, Society for Imaging Science and Technology, no. 1, pp. 333-338, 2006.
- [23] Y. Huo, F. Yang, L. Dong, and V. Brost, "Physiological inverse tone mapping based on retina response," *The Visual Computer*, vol. 30, no. 5, pp. 507-517, 2014.
- [24] B. Masia, A. Serrano, and D. Gutierrez, "Dynamic range expansion based on image statistics," *Multimedia Tools and Applications*, vol. 76, no. 1, pp. 631-648, 2017.
- [25] G.H. An, Y.D. Ahn, S. Lee, and S.J. Kang, "Perceptual brightness-based inverse tone mapping for high dynamic range imaging," *Displays*, vol. 54, pp. 1-8, 2018.
- [26] S. Choi, O.J. Kwon, J. Lee, and Y. Kim, "A JPEG backward-compatible image coding scheme for high dynamic range images," *Digital Signal Processing*, vol. 67, pp. 1-16, 2017.
- [27] Dev, S., Savoy, F.M., Lee, Y.H. and Winkler, S., 2018. High-dynamic-range imaging for cloud segmentation. arXiv preprint arXiv:1803.01071.